TÜBİTAK

Turkish Journal of Chemistry

http://journals.tubitak.gov.tr/chem/

Research Article

Turk J Chem
(2018) 42: 1217 – 1223

doi:10.3906/kim-1711-57

Phase transition of chemically synthesized FePt nanoparticles under high pressure

Telem ŞİMŞEK[1,*], **Özgür KARCI**[2,3], **Şadan ÖZCAN**[1]

[1]SNTG Laboratory, Department of Physics Engineering, Faculty of Engineering, Hacettepe University, Beytepe, Ankara, Turkey

[2]NanoMagnetics Instruments Ltd., Çankaya, Ankara, Turkey

[3]TÜBİTAK Space Technologies Research Institute, METU Campus, Çankaya, Ankara, Turkey

Received: 17.11.2017 • **Accepted/Published Online:** 14.05.2018 • **Final Version:** 11.10.2018

Abstract: We present the results of a study related to phase transformation of chemically synthesized FePt nanoparticles under high pressure from face-centered cubic into face-centered tetragonal structure. As-synthesized nanoparticles are around 4.5 nm and show superparamagnetic behavior at 300 K. After annealing under 60 bar pressure of hydrogen at 400 °C for 2 h, nanoparticles exhibit strong ferromagnetic behavior with 5391 Oe coercivity. Results show that high-pressure annealing lowers the decomposition temperature of the surfactants surrounding nanoparticles and partially hinders agglomeration arising from heat treatment. The promising ferromagnetic properties of the FePt nanoparticles after annealing under high pressure make them suitable for ultrahigh-density memory devices.

Key words: Chemical method, iron-platinum nanoparticles, magnetic data storage, phase transition

1. Introduction

Equiatomic FePt nanostructures with face-centered tetragonal (fct, $L1_0$) structure are very promising candidates for high-density magnetic storage devices beyond 1 Tbit/in^2 ($K_u = 7 \times 10^6\, J/m^3$).[1,2] Owing to their high magnetocrystalline anisotropy, the critical size at which FePt nanoparticles (NPs) become superparamagnetic at room temperature is as low as 3 nm.[3] In the fct structure, the Fe and Pt atoms form alternating layers along the c-axis and the alloy is ferromagnetic as a result of the hybridization between the 3d orbital of the Fe atoms and the 5d orbital of their Pt neighbors. Many attempts to produce FePt NPs have been made, and among them the chemical method has attracted much attention because as-made NPs have well-defined morphology and narrow size distribution.[4–9] However, as-synthesized FePt NPs exhibit an atomically disordered face-centered cubic (fcc, A_1) structure where iron (Fe) and platinum (Pt) atoms occupy the lattice positions randomly.[10] As a result of the disordered structure, NPs show superparamagnetic behavior at room temperature.[11] For this reason, a postthermal annealing process at about 580 °C is necessary to induce fcc into fct phase transition.[12] Furthermore, prolonged or high-temperature heat treatment is required to obtain fully transformed NPs. However, the organic ligands, which stabilize the NPs by surrounding the particles, decompose at around 400 °C, leading to undesired agglomeration or coalescence of the particles.[13,14] From the application point of view, particle agglomeration causes serious problems, such as decreased magnetic information storage density. In addition, agglomeration is an uncontrollable process that widens particle size distribution, leading to low signal-to-noise ratio of the magnetic devices and causing technological problems such as difficulty reading

*Correspondence: telem@hacettepe.edu.tr

the stored data back. Agglomerations may be overcome by using the well-known physical rule that the boiling point of a liquid varies depending on the surrounding environmental pressure. Thus, annealing the NPs under high pressure could increase the decomposition temperature of the surfactants surrounding them and completely or partially prevent the coalescence of NPs. Secondly, heat treatment under high hydrogen pressure is expected to decrease the phase transition temperature of FePt NPs from disordered fcc into ordered fct, as previously observed for bulk FePt films by Lai et al.[15] They reported that hydrogen atoms in the FePt structure promote the diffusion of Fe and Pt atoms by occupying the interstitial sites of FePt and inducing a local strain or an agitation that accelerates the ordering of FePt and decreases the phase transition temperature. In this regard, here we investigate the effect of heat treatment of chemically synthesized FePt NPs under high hydrogen pressure on the phase transition and sintering behavior of the NPs. For this purpose, chemically synthesized FePt NPs were drop-casted on Si(100) substrates and annealed under 60 bar of H_2 atmosphere, at 400 °C for 2 h. Results show that NPs were successfully transformed from fcc into fct structure with hard magnetic character as a result of heat treatment under high pressure with limited agglomeration.

2. Results and discussion

Figure 1a shows the X-ray diffraction (XRD) patterns of the as-synthesized and heat-treated FePt NPs along with Rietveld fits. All reflections are indexed, indicating the chemically disordered fcc crystal structure (space group: Fm3m) for the as-made sample where the lattice parameter is $a = 3.885 \pm 0.002$ Å.[16] As shown in the figure, annealing causes a shift of (111) reflection to higher degrees owing to the change in the lattice parameter, proving the phase transition from fcc into fct. Lattice parameters for the annealed FePt NPs are $a = 2.739 \pm 0.001$ Å and $c = 3.811 \pm 0.003$ Å, where $c/a = 1.39$. This ratio is in good agreement with the previous value experimentally derived for bulk FePt powder ($c/a = 1.36$).[17] In addition, the (110) superlattice reflection signifies the tetragonality of the ordered fct phase, which develops after annealing under high pressure. Crystalline sizes of the as-made and annealed sample were 4.7 nm and 9.2 nm, respectively. A transmission electron microscopy (TEM) micrograph of the as-made sample is shown in Figure 1b. Morphology of the NPs was nearly cubic with rounded edges. Average edge length of 92 particles, calculated statistically using ImageJ software, was 4.5 ± 0.3 nm (Figure 1b). The chemical composition of the as-made sample was confirmed by energy-dispersive X-ray spectroscopy (EDS) analysis. Measurements were obtained by spotting 5 different points on the sample with Si substrate and averaging the results. An EDS spectrum is shown in Figure 1c, showing the Fe and Pt content of the sample. The EDS profile also reveals Si content in the samples, due to the silicon substrate. Furthermore, the C peak in the EDS profile is related to the thin layer of C coating the samples prior to the measurement to induce conductivity. Results show that as-made NPs are nearly equiatomic $Fe_{50}Pt_{50}$.

The annealed sample was imaged using a low-temperature atomic force/magnetic force microscope (LT-AFM/MFM) (NanoMagnetics Instruments Ltd., Oxford, UK) at 300 K in PPMS.[18] In Figure 2a, a topography image of the sample shows how NPs are distributed on the silicon surface. The average height of the NPs was approximately 5 nm, which is compatible with the TEM results. However, the widths of the grains are larger than in the TEM image in Figure 2b, since the NPs are assembled together by means of dipolar interactions and the tip of the cantilever could not distinguish the individual particles because of the tip effects.

The room temperature hysteresis (M-H) curve of the as-made sample is given in Figure 3a. Zero coercivity and full saturation show that the as-made FePt NPs were superparamagnetic at room temperature. Observed

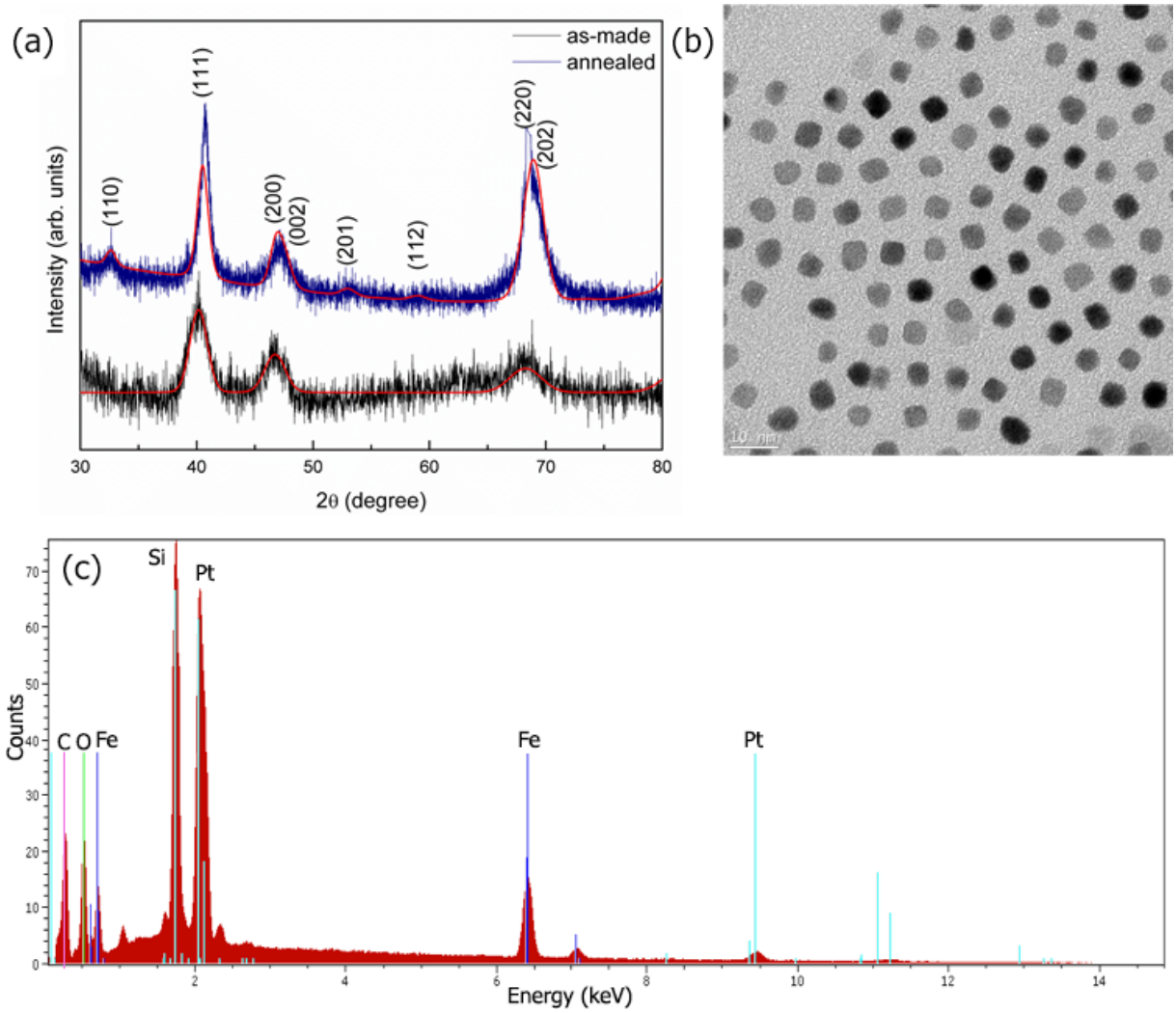

Figure 1. a) XRD patterns of as-made and annealed sample, b) TEM micrograph of the as-made sample, c) EDS spectrum of as-made sample.

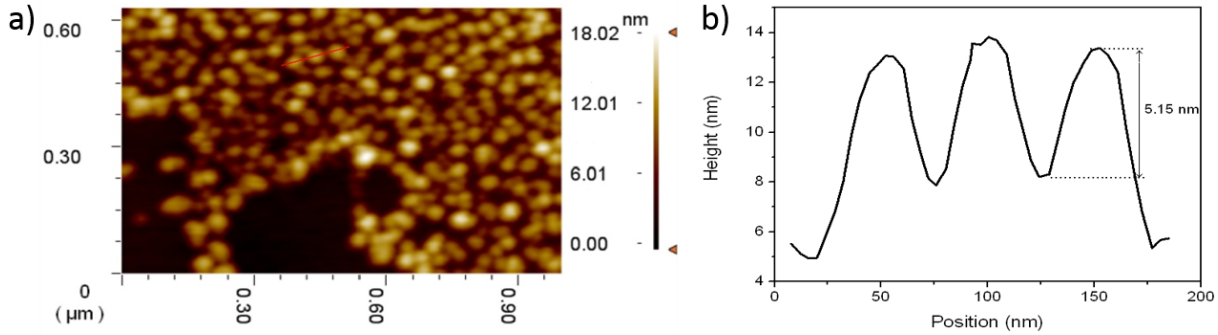

Figure 2. a) AFM image of the topography of the annealed NPs on the silicon substrate at 300 K, b) cross-section showing particle size.

superparamagnetic behavior originates from the disordered fcc phase and small particle size, as proven by structural analysis. Figure 3b shows the temperature dependence of the magnetization of the as-made FePt

NPs. In the measurement, the temperature was lowered to 10 K without applying a magnetic field (zero field cooled, ZFC) at first. At 10 K, a 500 Oe magnetic field was applied and magnetization of the sample was measured as a function of the increasing temperature. When the system reached room temperature, the sample temperature was again lowered to 10 K, but this time in the presence of a 500 Oe magnetic field (field cooled). The magnetization of the sample was measured as a function of decreasing temperature. A maximum at 35.6 K, which is called the blocking temperature (T_B), was observed in ZFC measurements, below which the superparamagnetic FePt NPs become ferromagnetic due to the reduced thermal energy.

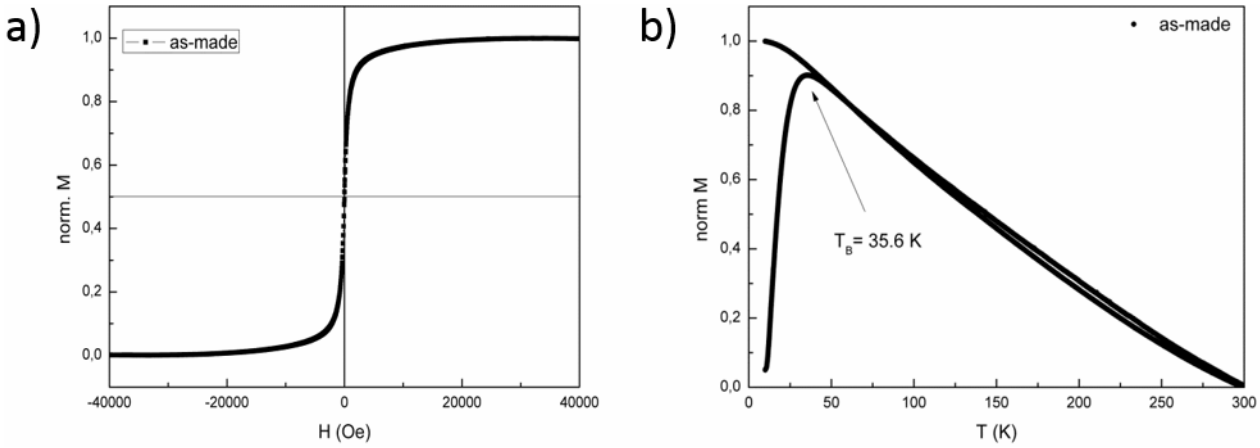

Figure 3. a) 300 K M-H curve of the as-made sample, b) M-T curve of as-made sample (H = 500 Oe).

The M-H curve of the annealed FePt NPs is depicted with an as-made sample for comparison in Figure 4. After annealing, a strong ferromagnetic signal was observed for FePt NPs with coercivity of 5391 Oe. The high coercivity shows that the phase transformation from fcc into fct structure was successful.

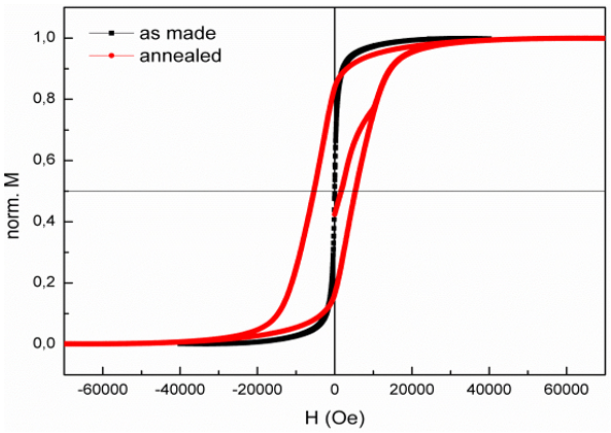

Figure 4. Room temperature hysteresis curves of the as-made and annealed FePt NPs.

A heat-treated sample under high pressure was imaged using MFM to see ferromagnetic signals from fct NPs (Figure 5). For MFM imaging, the microscope was operated in two-pass mode and Co-coated magnetic cantilevers (PPP-MFMR, NanoSensors Inc., Neuchâtel, Switzerland) were used. The cantilever was resonated in its resonance frequency (approximately 70 kHz) by means of a phase lock loop and oscillation amplitude

(10–50 nm) of the cantilever was used for feedback during scanning. In the first pass, the topography of the sample was obtained in semicontact mode AFM.[17] In the second pass, the magnetic tip was lifted by 10–100 nm to get rid of short-range forces. At this lift height, only long-range magnetic forces are dominant and cause frequency shift in the cantilever during raster scanning, which was recorded as the magnetic image of the sample. Figure 5a presents the NP cluster topography and the cluster size was approximately 50 nm. Figure 5b shows a magnetic dipole from the cluster and the phase shift was approximately 1.2°, which confirms a ferromagnetic signal coming from the NP cluster.

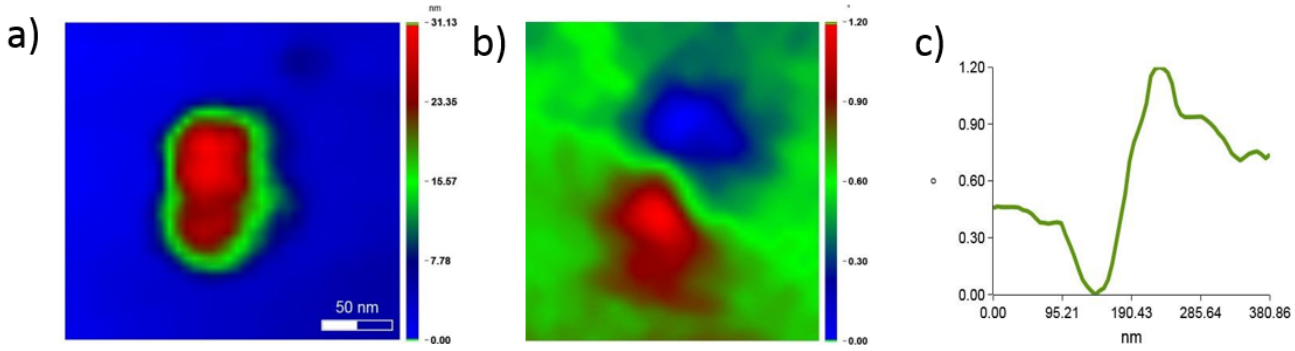

Figure 5. a) Topography image of an isolated NP cluster, b) MFM image of the cluster showing magnetic dipole, c) cross-section of the MFM image showing phase variation.

The sample was also imaged under an external magnetic field to see how magnetic domains behave with the applied field between 0 and 3 T. In Figure 6a, the variation in the image shows the random orientation of the magnetic domains of the fct NPs prior to applying an external magnetic field. When the field is increased up to 3 T, all of the magnetic domains are directed in the field direction, which is indicated by the uniform image texture in Figure 6b. In Figure 6c, the image shows the remnant magnetization of the fct NPs. In fact, the domain movements given in the figure are exactly what was expected from the M-H curves depicted in Figure 4, explaining the typical first quarter of the M-H hysteresis curve of a ferromagnetic material.

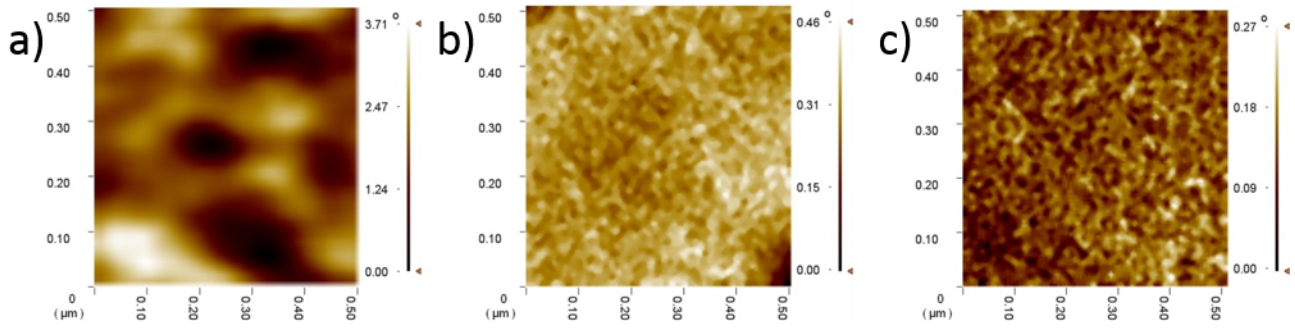

Figure 6. MFM images of the annealed FePt NPs: a) zero field image showing randomly oriented magnetic domains; b) 3 T image showing uniform distribution, indicating that all domains are directed with the field; c) zero field after 3 T image showing remnant magnetization, indicating that all the domains are frozen.

In conclusion in this work, structural and magnetic properties of FePt nanoparticles after annealing under high pressure are reported. We found that FePt NPs transform successfully from fcc into fct structure

after annealing at 400 °C. The FePt NPs show coercivity of 5391 Oe, which confirms the ordered fct structure with strong ferromagnetic signal. MFM images also confirmed the ferromagnetic signals. Results show that heat treatment under high pressure increases the decomposition temperature of the surfactants and fct FePt nanoparticles are successfully obtained by annealing at lower temperatures. However, annealing partially hinders particle agglomeration and particles grow up to 9 nm. The FePt NPs investigated here show good ferromagnetic behavior at room temperature that is suitable for high-density magnetic storage applications.

3. Experimental

To prepare FePt NPs, a combination of oleic acid and oleyl amine was used to stabilize the monodisperse FePt colloids and prevent oxidation. The synthesis is based on the reduction of $Pt(acac)_2$ (acac = acetylacetonate, $CH_3COCHCOCH_3$) and the decomposition of $Fe(CO)_5$ in benzyl ether.[19] The synthesis was carried out using standard airless procedures and commercially available reagents. In the synthesis, 0.5 mmol $Pt(acac)_2$ and 10 mL of benzyl ether were mixed with a magnetic stirrer in a round-bottomed reaction flask and purged with Ar for 30 min to remove O_2 and moisture. The flask was heated to 100 °C under 10 mL min^{-1} Ar flow and 1 mmol $Fe(CO)_5$, 4 mmol oleylamine, and 4 mmol oleic acid were injected into the mixture. The color of the solution became light yellow and turned orange as the Fe precursor was injected. After the OY and OA injection, the solution color changed to dark green. The mixture was further heated to 170 °C at a heating rate of 1.8 °C/min. Then the system was kept at this temperature for 3 h and the heat source was removed. The inert gas protection system was opened to the atmosphere after cooling to room temperature and the black precipitate was centrifuged with the addition of ethanol to remove the reaction byproducts. The as-synthesized NPs were dispersed in 20 mL of hexane. This solution of NPs was used to drop cast NPs on 3 × 3 mm^2 Si (100) substrates. Drop-casted FePt films were annealed under 60 bar pressure of H_2 at 400 °C for 2 h. The heat treatment was performed by using a Sievert-type volumetric hydrogen kinematic measurement system.

Structural properties of the samples were investigated with a Rigaku D-max B horizontal diffractometer (XRD) using CuKα radiation at a scanning rate of 0.02° s^{-1} (Neu-Isenburg, Germany). For chemical composition determination, EDS measurements were taken. Morphology and structure of the samples were characterized using TEM. Magnetic properties of the samples were characterized using the vibrating sample magnetometer module of PPMS. Both NP sizes and magnetic properties of the samples were imaged using a LT-AFM/MFM from NanoMagnetics Instruments (Oxford, UK).

References

1. Sun, S. H.; Murray, C. B.; Weller, D.; Folks, L.; Moser, A. *Science* **2000**, *287*, 1989-1992.
2. Weller, D.; Moser, A.; Folks, L.; Best, M. E.; Lee, W.; Toney, M. F.; Schwickert, M.; Thiele, J. U.; Doerner, M. F. *IEEE T. Magn.* **2000**, *36*, 10-15.
3. Rong, C. B.; Poudyal, N.; Chaubey, G. S.; Nandwana, V.; Skomski, R.; Wu, Y. Q.; Kramer, M. J.; Liu, J. P. *J. Appl. Phys.* **2007**, *102*, 043913.
4. Kang, S.; Harrel, J. W.; Nikles, D. E. *Nano Lett.* **2002**, *2*, 1033-1036.
5. Zeng, H.; Li, J.; Liu, J. P.; Wang, Z. L.; Sun, S. H. *Nature* **2002**, *420*, 395-398.
6. Shevchenko, E. V.; Talapin, D. V.; Schnablegger, H.; Kornowski, A.; Festin, O.; Svedlindh, P.; Haase, M.; Weller, H. *J. Am. Chem. Soc.* **2003**, *125*, 9090-9101.
7. Chen, M.; Liu, J. P.; Sun, S. *J. Am. Chem. Soc.* **2004**, *126*, 8394-8395.

8. Liu, C.; Wu, X.; Klemmer, T.; Shukula, N.; Yang, X.; Weller, D.; Roy, A. G.; Tanase, M.; Laughlin, D. *J. Phys. Chem. B* **2004**, *108*, 6121-6123.
9. Rong, C. B.; Nandwana, V.; Poudyal, N.; Li, Y.; Liu, J. P.; Ding, Y.; Wang, Z. L. *J. Phys. D* **2007**, *40*, 712-716.
10. Nguyen, H. L.; Howard, L. E. M.; Stinton, G. W.; Giblin, S. R.; Tanner, B. K.; Terry, I.; Hughes, A. K.; Ross, I. M.; Serres, A; Evans, J. S. O. *Chem. Mater.* **2006**, *18*, 6414-6424.
11. Sun, S.; Fullerton, E. E.; Weller, D.; Murray, C. B. *IEEE T. Magn.* **2001**, *37*, 1239-1243.
12. Harrell, J. W.; Wang, S.; Nikles, D. E.; Chen, M. *Appl. Phys. Lett.* **2001**, *79*, 4393-4395.
13. Sun, S. *Adv. Mater.* **2006**, *18*, 393-403.
14. Dai, Z. R.; Sun, S.; Wang, Z. L. *Nano Letters* **2001**, *1*, 443-447.
15. Lai, C. H.; Wu, Y. C.; Chiang, C. C. *J. Appl. Phys.* **2005**, *97*, 10H305.
16. Seehra, M. S.; Singh, V.; Dutta, P.; Neeleshwar, S.; Chen, Y. Y.; Chen, C. L.; Chou, S. W.; Chen, C. C. *J. Phys. D* 2010, *43*, 145002.
17. Lyubina, J.; Opahle, I.; Richter, M.; Gutfleisch,; Müller, K. H.; Schultz, L.; Isnard, O. *Appl. Phys. Lett.* **2006**, *89*, 032506.
18. Karcı, Ö.; Dede M.; Oral, A. *Rev. Sci. Inst.* **2014**, *85*, 103705.
19. Şimşek, T.; Özcan, Ş. *J. Magn. Magn. Mater.* **2014**, *351*, 47-51.